applied optics

2025 OIC Manufacturing "Road Runner" Challenge [Invited]

Daniel Poitras,[1,*] Amy L. Rigatti,[2] Michael R. Jacobson,[3] Catherine C. Cooksey,[4] Luke J. Sandilands,[1] and John J. Gilmore[5]

[1]National Research Council of Canada, Ottawa, Ontario K1A 0R6, Canada
[2]University of Rochester, Rochester, New York 14627, USA
[3]Optical Data Associates, Tucson, Arizona 85711, USA
[4]National Institute of Standards and Technology, Gaithersburg, Maryland 20899-8970, USA
[5]Optimax, Ontario, New York 14519, USA
*daniel.poitras@nrc.ca

Received 5 September 2025; revised 5 November 2025; accepted 6 November 2025; posted 6 November 2025; published 15 December 2025

Measurements of the fabricated optical filters submitted to the Manufacturing Challenge (MC) organized for Optica's Topical Meeting on Optical Interference Coatings held in Tucson, AZ, in May 2025, are presented. For this ninth MC, participants were asked to design and deposit, on a provided substrate, a filter with transmittance (T) and front- and back-reflectance (R) spectra (with light incident from the front and back, respectively) matching target values specified in the 400 nm to 1100 nm spectral interval. The challenge problem was selected to require at least one absorbing layer in the design in order to ensure a good performance. Six teams from three countries participated and submitted a total of 10 samples, all coated on both sides, with total thicknesses ranging from 3589 nm to 8088 nm and comprised of 31 to 135 layers. The entries were measured at four independent laboratories; the resulting merit function values obtained when comparing the measured spectra to the targets were used to rank the filters and determine a winner. In the analysis of the results, observations will be made about coating design, fabrication, and measurement. © 2025 Optica Publishing Group. All rights, including for text and data mining (TDM), Artificial Intelligence (AI) training, and similar technologies, are reserved.

https://doi.org/10.1364/AO.577764

1. INTRODUCTION

At Optica's last Conference on Optical Interference Coatings, *OIC2025*, the results of the 2025 OIC Manufacturing Challenge (MC) were presented, a triennial tradition since 2001 [1]. The MCs encourage the participants to design, fabricate, and measure filters prepared on identical blank substrates supplied by the organizers, with spectrophotometric properties that approach predetermined profiles, using the design, fabrication, and measurement tools of their choice. Although the competition and the comical target curves are entertaining, they are also educational. Participants can learn from addressing offbeat problems that differ from their demanding daily activities. The coating, optical, and general communities can get a sense of the state of the art and the current limitations in fabricating optical filters.

Techniques and tools for designing, fabricating, and measuring multilayer optical filters continue to advance. Over the years, even without knowing all the details behind the production of each sample, the results of this MC demonstrate this progress. A glance at previous MCs (see Section 7) indicates increasing filter complexity, with more layers and larger total thickness, depending on the problem. The relentless enhancement and adoption of deposition techniques, including purer materials, better thickness precision, *in situ* monitoring, online design re-optimization [2], and novel pre-deposition design robustness studies [3], all contribute to the better performance seen in this MC.

The target profile for the 2025 MC was chosen to induce the designers to include thin absorbing layers in their filters, with the expectation that it would be a high hurdle for all participants, regardless of their capabilities. We were grateful that our six courageous teams found the time and motivation to produce the samples that we analyzed in this work.

2. FORMULATION OF THE CHALLENGE

The profile for the *OIC2025* MC is shown in Fig. 1; it pays tribute to an Arizona celebrity, the avian "Arizona Road-Runner." Participants were invited to design, fabricate, and measure a filter with transmittance (T, at normal incidence) and reflectance (R, at 7.5° angle of incidence) spectra reproducing the outline of a sprinting bird. A list of numerical values for the targets is available online and as a supplement to this paper [4]. To optical thin-film designers, including the attendees to the *OIC2025*

Fig. 1. Target spectral curves for the OIC2025 optical coatings manufacturing challenge; T_0 represents the transmittance spectrum (at normal incidence), R_1 and R_2 are the reflectance spectra when measured from the front surface (side 1) and the back surface (side 2) of the filter, respectively (at 7.5° angle of incidence). (Photo credit: iStock/Frank Fichtmüller).

Conference, it is obvious that solutions must contain absorbers because (i) the sums of T and R spectra, on either side, are not close to unity (some light must be lost to absorption or scattering) and (ii) the two R spectra differ, which is only possible if absorption is introduced [5]. What is less known is that thin absorbing films can complicate the design and fabrication of filters, multiplying the number of preparation coatings and measurements during fabrication. In the following section, we will discuss these difficulties.

Each participating team fabricated its filters on identical substrates distributed to them by the organizers. Once completed, each team submitted their samples (a maximum of three per participant) to one of the organizers (A.R.), who tagged the filters with ID letters to maintain anonymity and repacked them in identical boxes. They were sent to Optical Data Associates and relayed to NRC, NIST, and Optimax, each producing a set of measurement data, and back to the organizers. The T and R spectra from the data sets were introduced into the following merit function (MF):

$$MF = \left\{ \frac{1}{N_0 + N_1 + N_2} \left[\sum_{i=1}^{N_0} \left(\frac{T_{0,i} - T_{0,i}^D}{\Delta T_{0,i}} \right)^2 + \sum_{i=1}^{N_1} \left(\frac{R_{1,i} - R_{1,i}^D}{\Delta R_{1,i}} \right)^2 + \sum_{i=1}^{N_2} \left(\frac{R_{2,i} - R_{2,i}^D}{\Delta R_{2,i}} \right)^2 \right] \right\}^{\frac{1}{2}}, \quad (1)$$

where $T_{0,i}$ and $T_{0,i}^D$ are the measured and target T values at normal incidence, while $R_{1,i}$ and $R_{1,i}^D$ are the measured and target R values as measured from the front side at 7.5° angle of incidence, and $R_{2,i}$ and $R_{2,i}^D$ are the measured and target R values as measured from the back side at 7.5° angle of incidence, at the specified wavelength λ_i; N_0, N_1, and N_2 are the total number of wavelengths defining $T_{0,i}^D$, $R_{1,i}^D$, and $R_{2,i}^D$ targets; $\Delta T_{0,i} = 0.001$, $\Delta R_{1,i} = 0.002$, and $\Delta R_{2,i} = 0.002$ are the T and R tolerances. All the T and R targets were defined as specular, assuming no light scattering. No assumption was made about the incident light polarization, assuming that it would not affect significantly the calculations and measurements. Note that all the T, R, and tolerance values are expressed as fractions between 0 and 1, not as percentages. The MF values calculated from Eq. (1) quantified sample performance. In the sections below, the samples and the performances will be described.

3. DISCUSSION OF THE CHALLENGE

This 2025 "Road Runner" problem was not the first involving both T and R spectra; we had previously posed the 2001 "Bow Lake" boggler [1] and the 2016 "Moose Head" mystery [6]. However, the Road Runner riddle is the first involving both front- and back-R spectra in addition to T; like the Moose Head matter, it requires absorbing layers; the Bow Lake business did not. As already stated in Ref. [6], the design and fabrication of filters with absorbing layers are not straightforward. These layers are often so thin that their complex refractive index changes with thickness due to film discontinuity, unstable growth dynamics, or size effects [7–9]. It was shown that this variation of n and k can significantly affect the expected multilayer performance [6]. The variation of the index can also make it difficult to monitor film thickness. Also, because these metals or semiconductors can oxidize, they can be modified by the deposition of adjacent oxide layers.

Figures 2(a) and 2(b) show a simple design for a dummy sample made in preparation for this challenge, using SiO_2, TiO_2,

and Al, and its expected performance. Figure 2(c) shows the measured performance of the dummy sample fabricated by one of the authors (D.P.); the resulting spectra clearly differ from the target curves and the expected performance: it looks more like a sketchy pelican!

This initial design had 10 layers and a total thickness of 573 nm, using SiO_2, TiO_2, and thin layers of Al as the absorbing material. An ion-beam sputtering system (Spector, from Veeco), equipped with a broadband optical thickness monitor, was used to deposit the coating. Figure 3 shows the sequence that led to the "Pelican" result. We see T spectra recorded for the first two TiO_2 and SiO_2 layers deposited before the first Al layer, for the Al layer itself, and for the subsequent TiO_2 layer, along with the calculated curves used for thickness determination. We fit only the thickness of the last layer deposited, assuming that the optical constants were those used in the design. We see how the unforeseen change of the Al optical constant led to an error in the thickness of that layer [Fig. 3(c)], shown as a lower-quality curve fit, and of the subsequent TiO_2 layer [Fig. 3(d)]. The remaining layer thicknesses were similarly affected, as well as the attempts to reoptimize and correct the design. Even adding layers and a coating on the back surface did not suffice to correct the situation. Using Eq. (1), we calculated an $MF \approx 65$; fortunately, in the following sections, we will see that all the participants did much better.

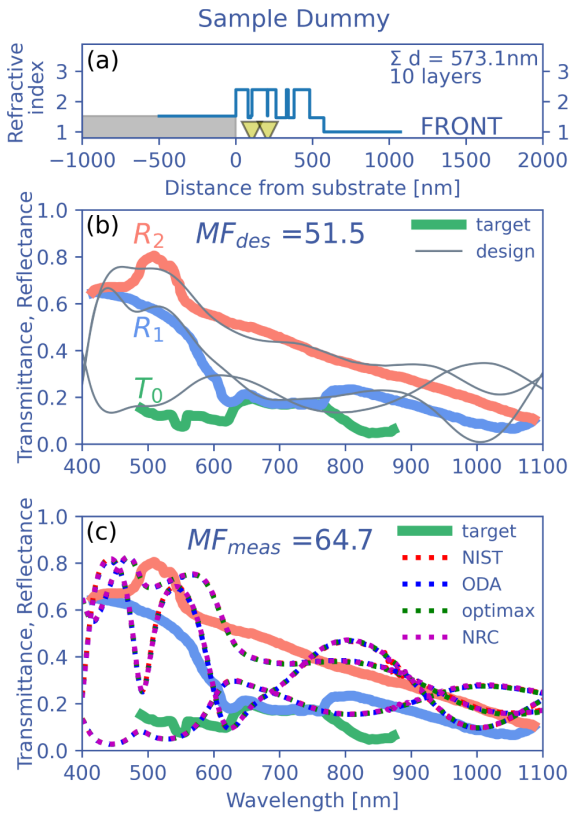

Fig. 2. Dummy sample fabricated in preparation for the challenge: (a) refractive index profile (at 750 nm) of a simple design, where the shaded area represents the substrate and the triangles show the positions of the thin absorbing layers inside the coating, (b) calculated expected spectra (transmittance and reflectance, as identified in Fig. 1), and (c) measured spectra after fabrication (with added layers to the design, including a back surface coating, in an attempt to correct for the first coating run mistakes and reduce the MF).

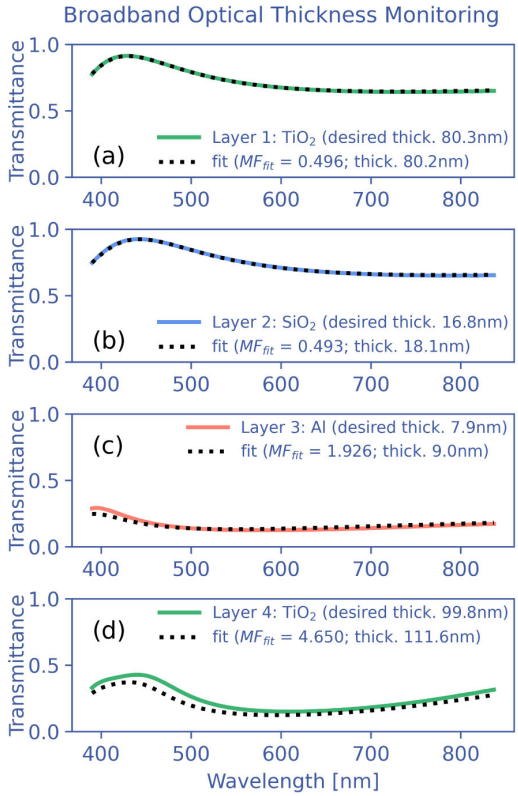

Fig. 3. *In situ* T spectra recorded during the fabrication of the dummy sample: (a) to (d), T taken after completed deposition of layers 1 to 4, respectively, with the best fit calculated using the design thickness values of the latest deposited layer, with previous deposited layers thicknesses fixed.

Interestingly, Fig. 3(d) also shows that the Al layer oxidized during the fabrication of the subsequent oxide layer. The measured T cannot be fitted by varying only the thickness of the top oxide layer, without reducing the thickness of the Al layer and adding an Al_2O_3 interface layer. One way to avoid this oxidation problem during fabrication is to protect it with a thin layer, such as amorphous Si, which, when oxidized, can easily be incorporated in the coating design without affecting the expected performance [10].

These three absorbing layer issues, the variation of the optical constant with thickness, its oxidation by the subsequent oxide layer, and the transition layer, are difficult to quantify when performing a prefabrication analysis to determine design robustness.

4. PARTICIPANTS AND EXPERIMENTAL INFORMATION

To our satisfaction, several teams—see Table 1—submitted samples.

Table 2 presents a description of the samples, with a comment about their fabrication provided by the participants. All included at least one absorbing layer, a metal (Ti or Al), or a suboxide (TaO_x or NbO_x), which can be thicker. Note that SiN_x was introduced as a protective film for Al layers in two of the

Table 1. List of Participants and Their Affiliation

Participating Team	Affiliation
Lucas Alves	Alluxa
Stefan Bruns	Fraunhofer IST
Zach Gerig	FiveNine Optics
Marc Lappschies, Jan Broßmann	Optics Balzers
Julien Lumeau, Fabien Lemarchand	Institut Fresnel
Gunnar Scott	Alluxa

entries. Also worth noting is that two pairs of samples shared the same designs, samples I and N, and samples S and T; the samples sharing the same design were fabricated by the same team, using the same deposition system, but in separate fabrication runs.

5. SAMPLE EVALUATION

The transmittance and reflectance spectra of the samples were measured at four independent laboratories; Table 3 describes their instruments and basic parameters. Instruments from three different manufacturers were involved, and measurements were performed with both direct/specular accessories and with integrating spheres. Because of the presence of thin metal and suboxide films prone to reacting with traces of oxygen, we were concerned with potential aging and degradation issues.

6. RESULTS AND DISCUSSION

In Figs. 4 and 5, the measured data for each entry are presented, along with the refractive index profile. The spectra provided by the participants are shown with those from the evaluation laboratories. We note that some participants provided a restricted data set sufficient for evaluating *MF* values but not covering the whole interval from 400 nm to 1100 nm; such cases are shown in Fig. 4(f) and Figs. 5(g)–5(i), where vertical lines show wavelength ranges covered.

One surprising observation about the designs is that all submissions had absorbing layers close to the coating surface; one would think that putting those "difficult" layers close to the substrate would offer more freedom to compensate for their n, k, and thickness deviations from the initial design by using remaining layers for design reoptimization. It could be a sign that the thicknesses and optical constants of the thin absorbing layers were generally well controlled, and that errors made on these layers could not be compensated by changing the thicknesses of the top remaining non-absorbing layers (an observation shared by one of the participants who used design reoptimization).

We also appreciate the close agreement among the spectra recorded by the participants and the four evaluation laboratories, which shows (i) general mastering and quality of the measurement techniques, particularly with R, (ii) no tangible scattering issues, spectra from instruments with integrating spheres matching those with specular setups and (iii) absence of aging effects (at least over the time of the evaluation period), even for those that include known reactive materials that were effectively protected by adjacent layers. The only notable discrepancies, mostly in the near-IR, were from Optimax's measurements of samples P and U, and that maybe due to a combination of factors that could involve a slight non-uniformity of the coatings and a different geometry (specular) for the measurements.

Table 4 and Fig. 6 display the data for all the entries. As for the estimation of errors in the *MF* values: in previous MCs, errors were deduced from the estimated measurement errors using an error propagation algorithm. In this MC, statistical standard deviations (σ) of the *MF* values calculated from the four data sets served as an error estimate of the experimental *MF* values. It gave larger numbers for the *MF* errors, partly due to errors from sample imperfections and the different instrument settings, not captured by the sole individual measuring instrument accuracies. We concluded that this approach provides a more realistic value.

Figure 6 offers a visual comparison of the results using a silhouette similar to "Wile E. Coyote" [11]), the hopeful but hapless harrier of the resourceful Road Runner, and his wayward weapon, an anvil, and where:

- The coyotes indicate the *MF* values before fabrication, evaluated from the designs provided by the participants, and
- The anvils show the average *MF* values calculated from the evaluation laboratories' data, with the size of the symbols proportional to the total filter thickness and with the blue and white sector areas proportional to front- and back-coating thicknesses.

Table 2. List of Submitted Samples, Anonymously Identified, with Their Front- and Back-Coating Thicknesses, Number of Layers, Absorbing Layer Information, and Additional Information about the Fabrication Process

	Thickness (nm)			Number of Layers			Absorbing Layer			
Sample	Side A	Side B	Total	Side A	Side B	Total	No.	Total Thick.	Materials (Bold = Absorbing)	Comment
E	4156.2	2589.0	6745.2	83	52	135	2	7.32	$Nb_2O_5/SiO_2/$**Ti**	Sputtering
F	3641.6	2643.6	6285.2	63	41	104	4	7.86	n/a	Sputtering
G	3969.5	3052.0	7021.5	47	43	90	4	33.9	$Ta_2O_5/SiO_2/$**TaO_x**	Suboxides
I	3953.3	3072.3	7025.6	51	42	93	2	22.02	$Nb_2O_5/SiO_2/$**NbO_x**	Suboxides
N	3953.3	3072.3	7025.6	51	42	93	2	22.02	$Nb_2O_5/SiO_2/$**NbO_x**	Suboxides
P	1729.4	1860.1	3589.5	17	14	31	2	16.4	$Nb_2O_5/SiO_2/SiN_x/$**Al**	Protective layer
S	3990.0	4098.3	8088.3	38	54	92	1	8.85	$TiO_2/SiO_2/$**Ti**	Ion-beam sputt.
T	3990.0	4098.3	8088.3	38	54	92	1	8.85	$TiO_2/SiO_2/$**Ti**	Ion-beam sputt.
U	1915.2	1809.4	3724.6	28	28	56	2	16.40	$Nb_2O_5/SiO_2/SiN_x/$**Al**	Protective layer
Y	2444.2	2854.8	5299.0	36	36	72	3	20.33	[a] n/a	Sputtering

[a]"n/a" means that this information was not available.

Table 3. Instruments Used by the Evaluation Labs for Evaluating the Submitted Samples (With Accessories and Measurement Accuracies)

	ODA	NIST	NRC	Optimax
Instrument	Agilent Cary 5000	Perkin Elmer Lambda 1050	Perkin Elmer Lambda 1050	Essen Optics Photon RT
Geometry	Hemispherical (integrating sphere)	Hemispherical (integrating sphere)	Hemispherical (integrating sphere)	Specular
T accuracy	±0.001	±0.001	±0.001	±0.001
R accuracy	±0.002	±0.002	±0.002	±0.002

Table 4. Comparison of the Samples *MF* Values, Ranked from the Lowest to the Highest MF_{avg} Value[a]

	Merit Function (*MF*)								
Sample	Design	Participant	ODA	NIST	NRC	Optimax	MF_{avg}	$\sigma(\pm)$	Rank
G	4.2	6.0	6.5	5.9	6.7	6.5	6.4	0.3	1
Y	4.0	7.7	6.8	7.3	6.9	7.3	7.1	0.2	2
I	4.2	8.3	8.7	8.0	8.1	9.3	8.5	0.5	3
N	4.2	8.9	10.4	10.3	9.7	11.4	10.4	0.6	4
F	3.8	16.0	13.3	13.0	13.9	14.3	13.6	0.5	5
S	5.3	15.2	14.7	15.3	15.1	15.4	15.1	0.3	6
T	5.3	15.5	15.6	15.1	14.3	15.4	15.1	0.5	6
E	0.2[b]	18.8	17.3	18.4	17.9	18.8	18.1	0.6	7
U	10.1	23.3	23.2	23.9	28.2	22.9	24.5	2.1	8
P	14.5	27.9	27.6	26.5	27.6	28.0	27.5	0.6	9

[a]The design values were reported by the participants, and the participants measured values were calculated from the spectra provided by the participants.
[b]Suspected calculation error.

One can see the discrepancies between expected (design, coyote symbols) and measured (anvil symbols) *MF* values, larger for samples with a larger *MF* (F, P, S, T, and U; the low design value of Sample E is due to a calculation error from one participant), and smaller for the remaining, better samples (G, I, N, and Y). Interestingly, a glance at Table 2 informs us that Samples G, I, and N, performing better than most other samples, all used thicker suboxide materials as absorbing layers (the absorbing material used in Sample Y was not revealed to us). We observe that samples P and U, with the largest values of *MF*, have the thinnest coatings (lower total physical thicknesses).

As Table 4 and Fig. 6 show, samples I and N, fabricated separately but using the same design, performed almost identically, while samples S and T, also sharing the same design, had a slight but noticeable difference in performance. With just two pairs of samples and no detailed information about their fabrication processes, it would be unwise to draw conclusions about the stability of each process or the robustness of the designs.

Overall, the 10 submitted samples were very good, with all *MF* values below 30, compared to our dummy sample with $MF \approx 65$. Nevertheless, comparing the *MF* values and considering the estimated errors, two samples, G and Y, were clearly better than the others, with Sample G being undoubtedly the best (not only on average but for each individual data set).

Therefore, as announced at the *OIC2025* conference in Tucson (May 2025), **Dr. Stefan Bruns** from the *Fraunhofer Institute for Surface Engineering and Thin Films (IST)*, who designed, fabricated, and measured Sample G, is declared the winner of the *OIC2025* MC. Looking again at his winning Sample G [Table 2 and Fig. 4(c)], we see that he used suboxide materials as absorbing layers, which allowed the usage of thicker films that are easier to control. Additionally, and it is an important fact revealed by Dr. Bruns, the suboxide layers were deposited using a sputtering target made of suboxide material (with the right stoichiometry), not a metal target. This means that no added oxygen was needed during the deposition of these layers, ensuring the stability of the process and the predictability of the suboxide layer composition and properties. It was a clever approach to avoid the difficulties linked to the deposition of thin absorbing layers, mentioned in Section 3.

7. CONCLUSION

Once again, the MC turned out to be challenging, entertaining, and instructive. With its spectral target curves combining *T* and *R* from both sides, the "Road Runner" problem was one of the most difficult so far. The impressive results from 10 entries show the enterprise of the participants and the advancing state of the art.

It is interesting to consider previous MCs and regard the progress in the sophistication and quality of the submissions. Figure 7 shows the evolution of the number of layers, total thickness, number of sides coated, and how closely fabricated (measured) sample performance achieved desired (design) performance (ratio MF_{meas}/MF_{des}). In these graphs, the challenges were divided into four categories related to their targets: *T* only, normal incidence (○), *T* only, oblique incidence, s- and p-polarization (∇), *T* and *R* (□), and color targets (Δ). We also plotted median curves to show the overall evolution of samples and the evolution of the distribution of samples around these median curves (50% of samples around the median versus 100% samples).

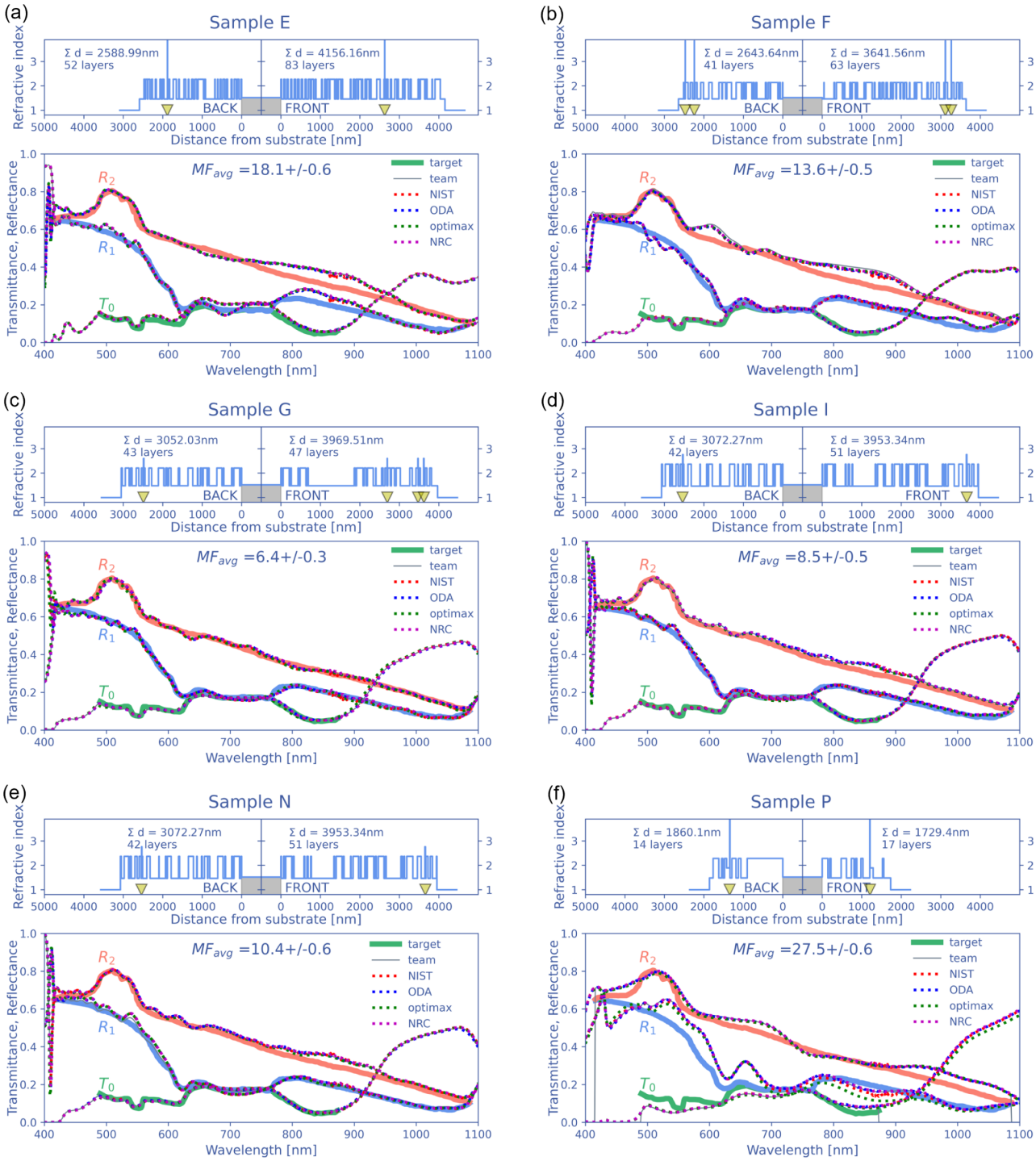

Fig. 4. Samples coating refractive index profiles at $\lambda = 750$ nm (top graphs, with triangles showing the positions of the thin absorbing layers), and measured performances (bottom graphs) [(a)–(f): Samples E to P, respectively].

Many observations can be made on the figure. It confirms, for example, that the 2025 "Road Runner" challenge was fairly difficult for all participants (it has a narrow distribution of sample numbers of layers and thicknesses); the required thin absorbing layers in the designs prevented any advantage for teams more skilled at controlling the deposition of thicker optical coatings with many hundreds of dielectric layers. The deposited absorbing layer's thicknesses and optical constants had a large impact on the performance that could not be compensated by using more dielectric layers, as opposed to problems using T only at normal incidence (as in 2022). Concerning problems using T only and normal incidence (○, years 2010, 2013, and 2022), we see that participants were increasingly able to deposit thick coatings with large numbers of layers (with more participants being able to do so in 2022). In general, we see a relatively clear

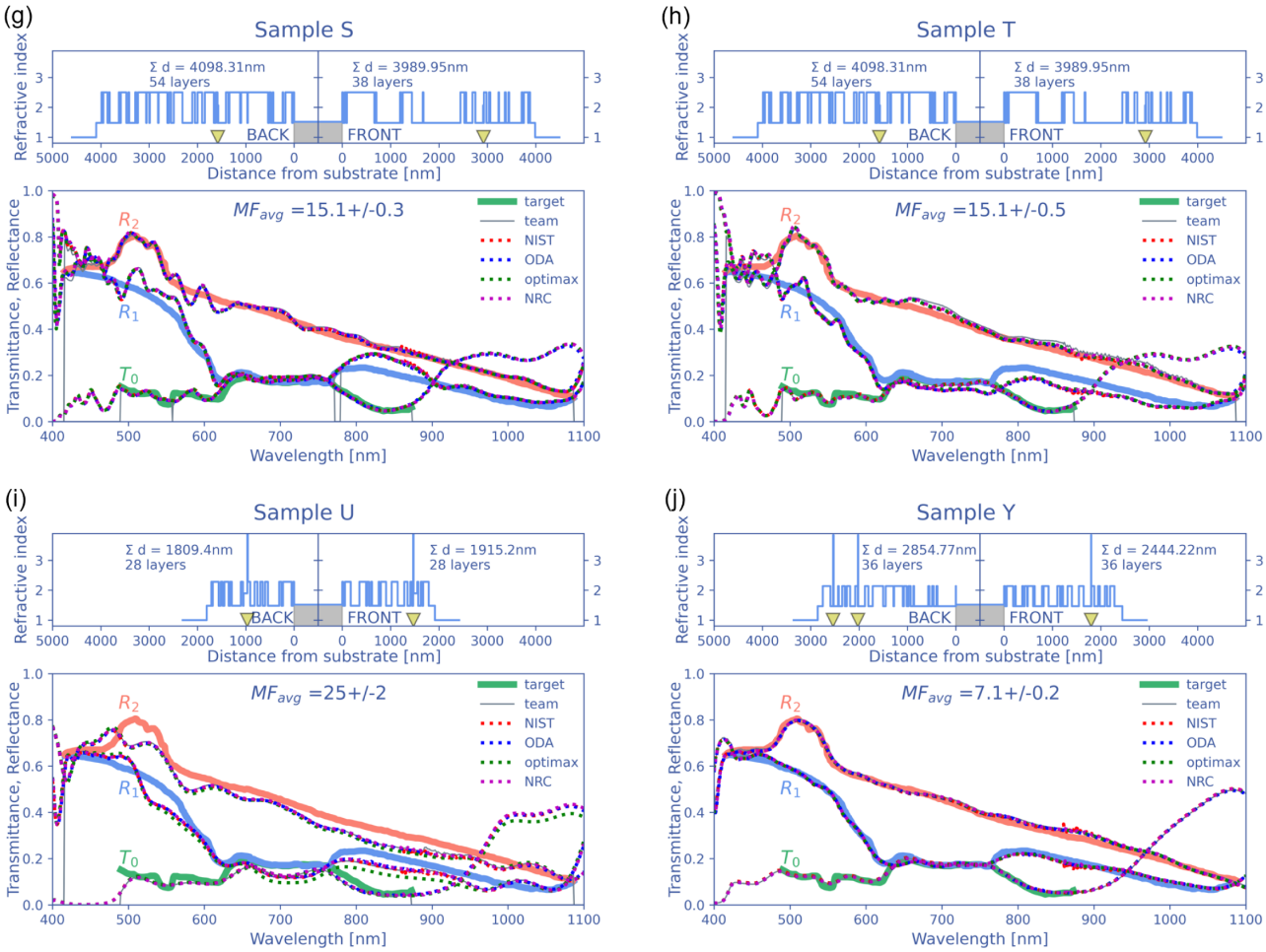

Fig. 5. (continuation of Fig. 4) Samples coating refractive index profiles and measured performances [(g)–(j): Samples S to Y, respectively].

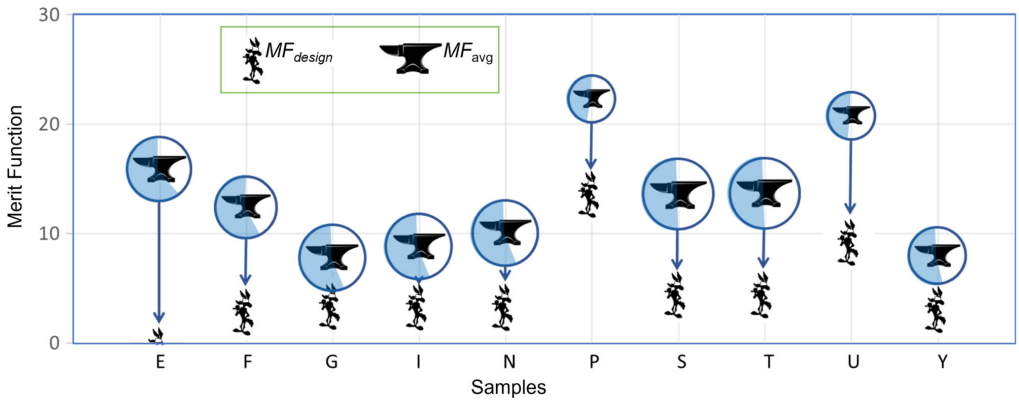

Fig. 6. Comparison of the merit function (MF) values of the submitted samples: the coyote symbols indicate (at its eye level) the design MF values provided by the participants; the anvil symbols indicate the average measured MF values (center of the circle), with the size of the anvil (and surrounding circle) proportional to the total thickness of the coating design, and the blue/white circle area ratio proportional to the front/back coating thickness ratio (see Tables 2 and 4 for the numerical values).

evolution of the number of layers and total thicknesses of the submitted samples.

Of course, the complexity of the coating solutions depends primarily on the type of problem to be solved. The challenges involving oblique incidence and/or R targets appear more equally difficult among participants (smaller variances in years 2001, 2004, 2007, 2016, 2019, and 2025). The problem of 2007 was distinct, involving colors (transmitted and reflected from both sides) and letting more freedom to the participants regarding the spectral properties of the samples.

In Fig. 7(d), we tried to quantify how good participants were at making filters that meet their own expectations, with properties close to their own designs. The ratio of measured-versus-design MF values seems to suggest that participants are

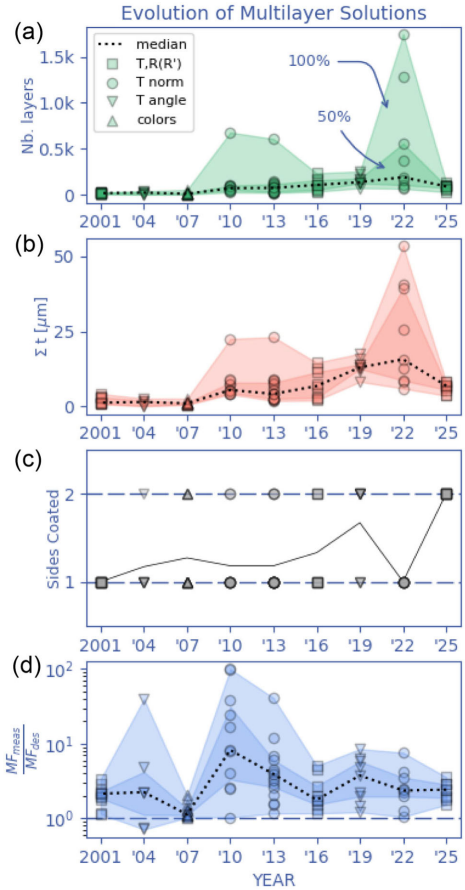

Fig. 7. Comparison of samples submitted to all manufacturing challenges (or problems) so far, from 2001 to 2025 [1,6,12–17]. (a) Number of layers, (b) total thickness, (c) one or both sides coated, and (d) how close the MF value is from the calculated value, ratio $MF_{\text{meas}}/MF_{\text{des}}$. In (a), (b) and (d) the dashed line represents the median value, the outside envelope includes all samples, while the inside envelope delimits 50% of the samples around the median. The problems were divided into categories involving: transmittance only, at normal incidence (○), transmittance only, as oblique angles (▽), transmittance and reflectance (□), and colors (△). In (c), the central curve represents the ratio of samples with two sides coated (adding 1 to make it fit between 1 and 2 on the graph). In (d), data from sample E were not considered.

generally getting better at fabricating what they design; even if the median of this ratio is still not reaching the ideal unity value. This is a sign that participants are improving both the fabrication and measurement of their coatings. It will be interesting to follow the evolution of these parameters in future challenges.

Acknowledgment. We wish to thank all the participants and their affiliations for dedicating effort and time (labor and machine) to solve this problem. Certain commercial equipment, instruments, or materials are reported in this paper to adequately specify the experimental procedure. Such identification is not intended as a recommendation or an endorsement by the NIST, nor is it intended to imply that the materials or equipment identified are necessarily the best available for the purpose.

Disclosures. The authors declare no conflicts of interest.

Data availability. Data for the target curves presented in this paper are available in Ref. [4]; other data underlying the results presented in this paper are available upon request.

REFERENCES

1. J. Dobrowolski, S. Browning, M. Jacobson, *et al.*, "Topical meeting on optical inferference coatings (OIC'2001): manufacturing problem," Appl. Opt. **41**, 3039–3052 (2002).
2. B. T. Sullivan and J. A. Dobrowolski, "Deposition error compensation for optical multilayer coatings. I. Theoretical description," Appl. Opt. **31**, 3821–3835 (1992).
3. T. V. Amotchkina, S. Schlichting, H. Ehlers, *et al.*, "Computational manufacturing as a key element in the design-production chain for modern multilayer coatings," Appl. Opt. **51**, 7604–7615 (2012).
4. D. Poitras, A. L. Rigatti, M. R. Jacobson, *et al.*, "OIC2025 'road runner' manufacturing challenge: target data and poster," figshare dataset (2025), https://doi.org/10.6084/m9.figshare.30402418.v1.
5. O. Heavens, "Optical properties of thin films," Rep. Prog. Phys. **23**, 1–65 (1960).
6. D. Poitras, L. Li, M. Jacobson, *et al.*, "Manufacturing problem contest," Appl. Opt. **56**, C1–C10 (2017).
7. J. Kim, H. Oh, M. Seo, *et al.*, "Generation of reflection colors from metal–insulator–metal cavity structure enabled by thickness-dependent refractive indices of metal thin film," ACS Photonics **6**, 2342–2349 (2019).
8. A. Sotsky, E. Chudakov, and L. Sotskaya, "The anomalous skin effect in metallic films," J. Appl. Spectrosc. **91**, 812–825 (2024).
9. H. Kangarlou and M. M. Aghgonbad, "Influence of thickness on optical properties of titanium layers," Opt. Spectrosc. **115**, 753–757 (2013).
10. B. Sullivan and K. Byrt, "Metal/dielectric transmission interference filters with low reflectance. 2. Experimental results," Appl. Opt. **34**, 5684–5694 (1995).
11. Wikipedia contributors, "Wile E. Coyote and the Road Runner—Wikipedia, the free encyclopedia," 2025, https://en.wikipedia.org/w/index.php?title=Wile_E._Coyote_and_the_Road_Runner.
12. J. A. Dobrowolski, S. Browning, M. R. Jacobson, *et al.*, "2004 Optical Society of America's topical meeting on optical interference coatings: manufacturing problem," Appl. Opt. **45**, 1303–1311 (2006).
13. J. A. Dobrowolski, S. Browning, M. Jacobson, *et al.*, "2007 topical meeting on optical interference coatings: manufacturing problem," Appl. Opt. **47**, C231–C245 (2008).
14. J. A. Dobrowolski, L. Li, M. Jacobson, *et al.*, "2010 topical meeting on optical interference coatings: manufacturing problem," Appl. Opt. **50**, C408–C419 (2011).
15. L. Li, J. A. Dobrowolski, M. Jacobson, *et al.*, "Broadband transmission filters from the 2013 optical interference coatings manufacturing problem contest," Appl. Opt. **53**, A248–A258 (2014).
16. D. Poitras, L. Li, M. R. Jacobson, *et al.*, "2019 topical meeting on optical interference coatings: manufacturing problem contest," Appl. Opt. **59**, A31–A39 (2020).
17. D. Poitras, P. Ma, M. R. Jacobson, *et al.*, "2022 optical interference coatings conference: manufacturing problem contest," Appl. Opt. **62**, B104–B111 (2023).